

Zonal Flow and Zonal Magnetic Field Generation by Finite β Drift Waves: A Theory for Low to High Transitions in Tokamaks

P. N. Guzdar and R. G. Kleva

Institute for Plasma Research, University of Maryland, College Park, Maryland 20742

A. Das and P. K. Kaw

Institute for Plasma Research, Bhat, Gandhinagar, Gujarat

(Received 8 November 2000; published 15 June 2001)

The understanding of low to high (L-H) transition in tokamaks has been an important area of investigation for more than a decade. Recent 3D finite β simulations of drift-resistive ballooning modes in a flux tube geometry by Rogers *et al.* [Phys. Rev. Lett. **81**, 4396 (1998)] have provided a unique parametrization of the transition in a two-dimensional phase space. Comparison of the threshold curve in this phase space with data from ASDEX and C-MOD has shown very good agreement. In this Letter we provide a simple theory, based on the generation of zonal flow and zonal magnetic field in a finite-beta plasma, which explains this threshold curve for L-H transition in tokamaks.

DOI: 10.1103/PhysRevLett.87.015001

PACS numbers: 52.35.Kt, 52.30.Cv, 52.55.Fa

The observation of the low to high confinement (L-H) transition in tokamaks heralded significant optimism for achieving the goal of fusion in a laboratory plasma [1–3]. More recently the observation of enhanced confined modes in all the major devices has also added to the optimism [4,5]. As a consequence, understanding of this remarkable self-organization of the tokamak plasma to these good confinement regimes is an important area of research. Central to all these enhanced confinement regimes, be they in the edge region or the core region of the plasma, is the generation of sheared flows or zonal flows, which are believed to be responsible for suppressing fluctuations and inhibiting transport. Thus it is important to understand the mechanisms for the generation of shear flow.

We have recently reviewed the study of shear flow generation in fluids and plasmas, with a focus on the linear instability analysis [6], and therefore will defer the reader to this paper for details and relevant references. Besides these studies in which the dominant mechanism for the generation of the flow is related to the nonlinear mode coupling, other mechanisms, like ion orbit loss [7] and the anomalous Stringer-Winsor [8] and anomalous viscosity mechanisms [9], which rely on toroidal geometry, and more recently the two-fluid self-organized singular layer model [10], have also been investigated. A very recent review by Connor and Wilson [11] gives an excellent overview of the observations and theories for L-H transition in tokamaks.

The modeling of L-H transitions in tokamak plasmas has also been an active area of research. Starting with the work of Guzdar *et al.* [12], Rogers *et al.* [13] and Xu *et al.* [14] have systematically developed edge models for studying the cause of anomalous transport in the L phase and the subsequent improvement in confinement in the H phase. Rogers *et al.* [13], in their finite-beta simulations of drift-resistive ballooning modes, have identified a two-

dimensional parameter space involving α_{MHD} and α_D in which the edge plasma displays dramatic changes in transport. The first parameter $\alpha_{\text{MHD}} = \beta q^2 R/L_p$, with safety factor q , major radius R , pressure gradient scale length L_p , and ratio β of the plasma pressure to the magnetic pressure, is the standard MHD parameter identified for the onset of ideal ballooning modes. The second parameter α_D is the dimensionless diamagnetic parameter. It is the ratio of the diamagnetic drift frequency $\rho_s c_s/L_0 L_n(1 + \tau)$ to the ideal growth rate $c_s/\sqrt{RL_n}/2$. Here ρ_s is the ion Larmor radius with the electron and ion temperature, c_s is the ion acoustic velocity, L_0 is the characteristic scale length [9,10] of the drift-resistive ballooning instability, L_n is the density gradient scale length, and $\tau = T_i/T_e$ is the ratio of ion to electron temperature. From their simulations, they showed that for small α_D and α_{MHD} below the ideal limit, the anomalous transport from resistive ballooning modes is very large and increases with α_{MHD} . They interpret the computed large levels of transport to be responsible for the density limit in tokamaks. However, for finite α_D , as α_{MHD} is increased, there is a transition from a poorly confined state (L mode) to a good confined state (H mode). This simulation is the first to identify a beta dependence for the L-H transition. Also subsequent comparison with data from ASDEX [15], C-Mod [16], and DIII-D [17] showed that the numerically computed shape of the boundary curve for the L-H transition was in good agreement with the observations. However, the constant associated with the curve was different for the three cases. In this Letter we report a simple theory for the generation of zonal flow and zonal magnetic field in a finite-beta plasma. Recently Gruzinov *et al.* [18] have studied the problem of zonal field generation by using the wave-kinetic approach. Their focus has been on understanding the dynamo problem. We present here the coherent modulational instability analysis and its

implications to L-H transitions. Furthermore, we show how this instability mechanism can lead to a threshold curve similar to the one obtained by Rogers *et al.* [13].

The basic equations used have been derived by Zeiler *et al.* [19]. They are

$$\frac{dn}{dt} = \frac{c_s^2}{\Omega_i} \frac{1}{L_n} \frac{\partial \phi}{\partial y} - \nabla_{\parallel} J = 0, \quad (1)$$

$$\frac{c_s^2}{\Omega_i^2} \nabla_{\perp} \cdot \frac{d}{dt} \nabla_{\perp} \phi - \nabla_{\parallel} J = 0, \quad (2)$$

$$\frac{\partial \psi}{\partial t} + \frac{c_s^2}{\Omega_i} \frac{1}{L_n} \frac{\partial \psi}{\partial y} - v_A \nabla_{\parallel} (\phi - n) = 0, \quad (3)$$

with

$$J = v_A \frac{c_s^2}{\Omega_i^2} \nabla_{\perp}^2 \psi, \quad (4)$$

$$\nabla_{\parallel} = \nabla_{\parallel 0} + \frac{c_s^2 R_0}{\Omega_i v_A} \nabla \zeta \times \nabla \psi \cdot \nabla, \quad (5)$$

and

$$\frac{d}{dt} = \frac{\partial}{\partial t} + \frac{c_s^2 R_0}{\Omega_i} \nabla \zeta \times \nabla \phi \cdot \nabla. \quad (6)$$

$n = \tilde{n}/n_0$, $\phi = e\tilde{\phi}/T_e$, and $\psi = (\Omega_i v_A/c_s^2 B_0)\tilde{\psi}$ are the normalized perturbed density, electrostatic potential, and parallel vector potential, respectively. In these equations R_0 is the major radius, Ω_i is the ion gyroradius, c_s is the ion acoustic speed computed with only the electron temperature, L_n is the density gradient scale length, v_A is the Alfvén velocity, and ζ is the toroidal angle. Here a few comments are in order. We have neglected the curvature terms as well as any dissipation effects. The curvature terms play a role in destabilizing the finite-beta drift waves observed in the simulations, whose stability we investigate.

In the linear analysis that follows, the implicit assumption is that we have a large amplitude finite-beta drift wave. All the three quantities n , ϕ , and ψ associated with this pump wave can be written as

$$\xi = \xi_0 \exp(ik_y y + ik_{\parallel} z - i\omega_0 t), \quad (7)$$

where ξ represents any one of the three quantities. To investigate the stability of this wave to the generation of shear/zonal flow (ϕ_s) and zonal magnetic field (ψ_s), the perturbed quantities can be represented as

$$\begin{aligned} \xi &= \xi_s \exp(ik_x x - i\omega t) \\ &+ \xi_+ \exp(ik_x x + ik_y y + ik_{\parallel} z - i\omega_+ t) \\ &+ \xi_- \exp(ik_x x - ik_y y - ik_{\parallel} z - i\omega_- t), \end{aligned} \quad (8)$$

where $\omega_{\pm} = \omega \pm \omega_0$. The first term represents the shear/zonal flow (ϕ_s) and zonal magnetic field (ψ_s). The zonal magnetic field occurs only in a finite-beta plasma.

The second and third terms represent all three perturbed quantities for the sidebands which couples the shear flow and zonal magnetic field to the pump drift wave. The wave number and frequency matching conditions determine the spatial and temporal dependence assigned to the \pm sidebands. Because of the dispersive character of the drift waves, the two sidebands are nonresonant and are equally important. This four-wave coupling is therefore the simplest model representing the generation of shear flow and zonal magnetic field by a finite-beta drift wave. This representation is the local version of that used by Chen *et al.* [20] and the complex representation of that used by Guzdar *et al.* [6]. Here ω_0 is the mode frequency satisfying the dispersion relation for drift and drift-Alfvén waves,

$$1 + k_y^2 \rho_s^2 - \frac{\omega_*}{\omega_0} - \frac{\omega_0(\omega_0 - \omega_*)}{k_{\parallel}^2 v_A^2} = 0. \quad (9)$$

Here $\omega_* = k_y \rho_s c_s / L_n$ is the electron diamagnetic frequency. In this Letter we will consider only the shear flow and zonal field generation by the drift-wave branch and address the issue of shear flow generation by drift-Alfvén waves in a later publication.

The four coupled equations for zonal flow ϕ_s , zonal field ψ_s , and the sidebands ϕ_{\pm} lead to the following dispersion relation for shear flow/zonal field generation:

$$\begin{aligned} \omega^2 - \Delta^2 &= -2\gamma_s^2 \left[M_A \left(1 - \frac{\omega_0^2}{k_{\parallel}^2 v_A^2} \right) \right. \\ &\quad \left. + M_B (k_x \rho_s)^2 \left(\frac{\omega_0}{k_{\parallel} v_A} \right)^2 \right], \end{aligned} \quad (10)$$

where $\Delta = k_x^2 \rho_s^2 \omega_0 / A$, and

$$\begin{aligned} M_A &= \left[1 - 2 \frac{\omega_0}{k_{\parallel}^2 v_A^2} \left(\omega_0 - \frac{\omega_*}{2} \right) \right. \\ &\quad \left. + \frac{k_x^2 - k_y^2}{k_{\perp}^2} \left(1 - \frac{\omega_*}{\omega_0} - k_x^2 \rho_s^2 \right) \right] / A, \end{aligned} \quad (11)$$

$$M_B = - \left[\frac{2k_y^2}{k_{\perp}^2} \left(1 - \frac{\omega_*}{\omega_0} + k_y^2 \rho_s^2 \right) \right] / A, \quad (12)$$

$$A = 1 + k_{\perp}^2 \rho_s^2 - \frac{3\omega_0(\omega_0 - 2\omega_*/3)}{k_{\parallel}^2 v_A^2}. \quad (13)$$

Δ is the frequency shift between the pump wave and the sidebands. This arises due to the dispersive nature of drift waves. Here $k_{\perp}^2 = k_x^2 + k_y^2$ and $\gamma_s = \Gamma|\phi_0| = (k_x k_y c_s^2 / \Omega_i) |\phi_0|$ is the maximum growth rate for the shear flow instability for the electrostatic case.

This dispersion relation is the finite-beta slab version of Eq. (10) in the work of Chen *et al.* [20] and also includes the large mode-number limit because of the terms associated with the nonlinear polarization drift in the drift-wave components. If we examine this dispersion relation, we find that there are two distinct finite β effects. The first such effect, which appears in the matrix element M_A is due

to the finite β associated with the pump drift wave and the sidebands. The second finite-beta effect arises because of the zonal field ψ_s . The nature of the coupling shows that the zonal flow and the zonal field are on the same footing, both being driven by the pump wave and the two sidebands.

To solve the dispersion relation for the zonal flow/zonal field [Eq. (10)], it is first necessary to solve the dispersion relation for the pump drift [Eq. (9)]. Normalizing the frequency ω_0 to the drift frequency ω_* , and assuming $k_{\parallel} \sim (qR)^{-1}$, the normalized dispersion relation [Eq. (9)] becomes

$$1 + k_y^2 \rho_s^2 - \frac{1}{\Omega_0} - \Omega_0 k_y^2 \rho_s^2 \hat{\beta} (\Omega_0 - 1) = 0. \quad (14)$$

Subsequently the growth rate for the shear/zonal flow and field [Eq. (10)] becomes

$$\gamma = (k_x \rho_s) (k_y \rho_s) [M_A (1 - \Omega_0^2 k_y^2 \rho_s^2 \hat{\beta}) + M_B \Omega_0^2 k_x^2 \rho_s^2 k_y^2 \rho_s^2 \hat{\beta} - \hat{\Delta}^2]^{1/2}. \quad (15)$$

Here $\Omega_0 = \omega_0/\omega_*$, $\hat{\beta} = \beta(qR/L_n)^2/2$, and $\hat{\Delta}^2 = (1/2)(\rho_s/L_n)^2(k_x \rho_s)^2 \Omega_0^2/|\phi_0|^2$. Also the growth rate has been normalized to $\Omega_i|\phi_0|$. These normalizations show that there are four dimensionless parameters, (1) $k_y \rho_s$, (2) $k_x \rho_s$, (3) $\hat{\beta}$, and (4) $|\phi_0|L_n/\rho_s$. The simple dispersion relation [Eq. (15)] for the growth rate yields very interesting results for the generation of shear/zonal flow and field.

Shown in Fig. 1 are the dispersion curves for the drift-wave branch for $k_y \rho_s = 0.1$ (solid line), $k_y \rho_s = 0.25$ (dashed line), and $k_y \rho_s = 0.5$ (dash-long-dashed line) as a function of $\hat{\beta}$. As seen from the plots, the inclusion of finite beta strongly reduces the frequency of the drift wave. Using these eigenfrequencies, we now compute the growth rate for the shear/zonal flow and field.

For the drift-wave pump mode, Fig. 2 shows the growth rate of the maximally growing mode (maximized over $k_x \rho_s$) as a function of $\hat{\beta}$ for $k_y \rho_s = 0.1$ (solid line), $k_y \rho_s = 0.25$ (dashed line), and $k_y \rho_s = 0.5$ (dash-long-dashed line) for $|\phi_0| = \rho_s/L_n$. For $k_y \rho_s = 0.1$, the stabilizing influence of the finite-beta effects associated with

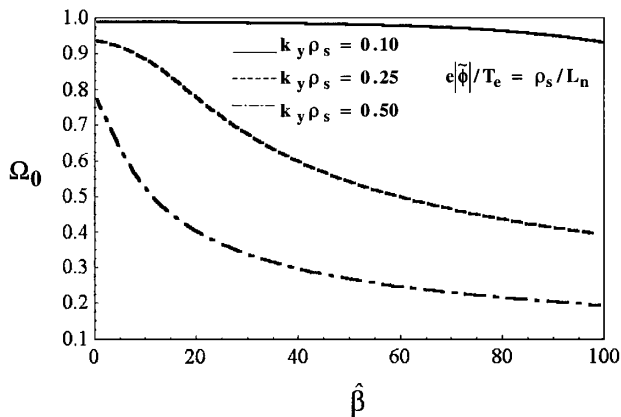


FIG. 1. Eigenfrequency Ω_0 for drift-wave branch versus $\hat{\beta}$ for $|\phi_0| = \rho_s/L_n$, $k_y \rho_s = 0.1$ (solid line), $k_y \rho_s = 0.25$ (dashed line), and $k_y \rho_s = 0.5$ (dash-long-dashed line).

the drift wave and the sidebands dominates, and the maximum growth rate decreases as a function of $\hat{\beta}$. However, for the larger $k_y \rho_s$ this stabilization occurs for small $\hat{\beta}$ and the destabilizing influence of the zonal field coupling dominates for larger $\hat{\beta}$. The minimum of this maximized growth rate shifts to lower $\hat{\beta}$ as $k_y \rho_s$ increases.

We now argue that the threshold for the onset of L-H transition is the minimum point of the curves. Namely,

$$\left. \frac{d\gamma}{d\hat{\beta}} \right|_{\hat{\beta}=\hat{\beta}_c} = 0, \quad \left. \frac{d^2\gamma}{d\hat{\beta}^2} \right|_{\hat{\beta}=\hat{\beta}_c} > 0. \quad (16)$$

This can be understood as follows. At $\hat{\beta} = \hat{\beta}_c$, the shear flow/zonal field causes stabilization of the turbulence and as the density steepens $\hat{\beta}$ increases. This increases the growth rate of the zonal flow/field instability, thereby further enhancing the stabilization of the turbulence and the steepening of the density gradient. On the other hand, for $\hat{\beta} < \hat{\beta}_c$, even though the zonal flow instability is present, the steepening of the density gradient cannot be sustained since it causes the growth rate for the flow to decrease, thereby allowing the turbulence to grow and cause more transport.

The next step is to establish a threshold condition. Figure 3 is a plot of the quantity $\Lambda_c = (k_y \rho_s)^2 \hat{\beta}_c$ versus $k_y \rho_s$ for $e|\tilde{\phi}_0|/T_e = (1/2)\rho_s/L_n$ (diamond), $e|\tilde{\phi}_0|/T_e = \rho_s/L_n$ (circle), $e|\tilde{\phi}_0|/T_e = 2\rho_s/L_n$ (square). In fact, for $e|\tilde{\phi}_0|/T_e \geq 2\rho_s/L_n$, the values of $(k_y \rho_s)^2 \hat{\beta}_c$ versus $k_y \rho_s$ are almost identical to those for $e|\tilde{\phi}_0|/T_e = 2\rho_s/L_n$ (square). For the pump amplitude $e|\tilde{\phi}_0|/T_e \geq 1/2\rho_s/L_n$, and $k_y \rho_s$ varying over a range of five, the value of $\Lambda_c = (k_y \rho_s)^2 \hat{\beta}_c$ is tightly bound between 1.7 and 2.1. Thus we can state the threshold criterion as $(k_y \rho_s)^2 \hat{\beta}_c = 1.7-2.1$.

If we assume that $k_y = 2\pi/L_0$, where L_0 is the characteristic scale length defined in the work of Guzdar *et al.* [12] and later in the work of Rogers *et al.* [13], then $(k_y \rho_s)^2 \hat{\beta}_c = 4\pi^2(1 + \tau)\alpha_{\text{MHD}}\alpha_D^2/(1 + \tau + \eta_e + \tau\eta_i)$. Thus for $\tau = T_i T_e = 1$, $\eta_e = d \ln T_e / d \ln n = 1$, $\eta_i = d \ln T_i / d \ln n = 1$ as used in the simulation of Rogers

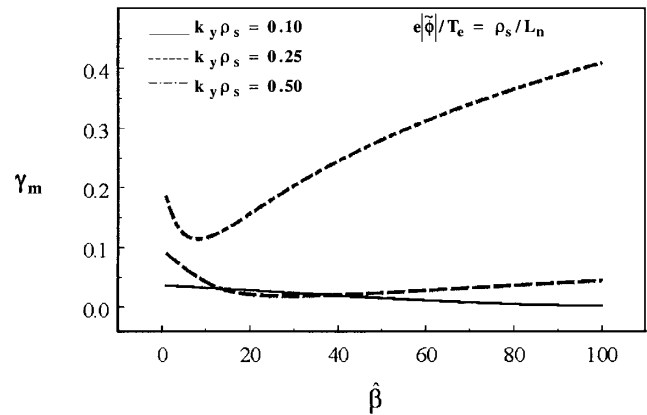


FIG. 2. Maximum growth rate γ_m versus $\hat{\beta}$ for drift-wave pump with $|\phi_0| = \rho_s/L_n$. The different curves are for $k_y \rho_s = 0.1$ (solid line), $k_y \rho_s = 0.25$ (dashed line), and $k_y \rho_s = 0.5$ (dash-long-dashed line).

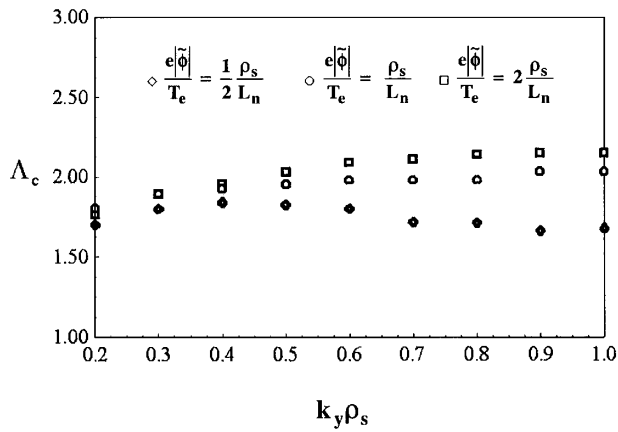


FIG. 3. $\Lambda_c = (k_y \rho_s)^2 \hat{\beta}_c$ versus $k_y \rho_s$ for $e|\tilde{\phi}_0|/T_e = (1/2)\rho_s/L_n$ (diamond), $e|\tilde{\phi}_0|/T_e = \rho_s/L_n$ (circle), and $e|\tilde{\phi}_0|/T_e = 2\rho_s/L_n$ (square).

et al. [13], this threshold condition therefore translates to $\alpha_{\text{MHD}}\alpha_D^2 = 0.085\text{--}0.12$. We fitted our $\alpha_{\text{MHD}}\alpha_D^2$ scaling to the numerically obtained L-H transition curve by Rogers *et al.* [13] and found the scaling was in agreement with their results; however, the constant for their data was 0.35. As mentioned earlier, for comparison of the Rogers *et al.* [13] result with the DIII-D and C-MOD data, their constant had to be adjusted to lower values by two to four. This was due to the differences in the definitions of α_D used in the experimental studies as well as the difference in the values of τ , η_e , and η_i between the simulations and experiments. If we use $\eta_i = \eta_e = 2$ and $\tau = 1$, for C-MOD, our theoretical model agrees well with the data set presented by Hubbard *et al.* [16] in their Fig. 3. Also for the DIII-D case, since our constant is smaller, our analytic curve is in better agreement with the DIII-D data shown in Fig. 8 [17]. In reality it is necessary to measure the gradients of the electron and ion temperature as well as the density to compute the constant more accurately. Further improvement in our model including finite ion temperature effects and more detailed comparison with simulations and experimental data will be the subject of future work. Thus we conclude that the L-H transition is triggered by shear flow/zonal magnetic field suppression of turbulence and the sustainment of the flow and magnetic field by the steepening of the density gradient.

This work was supported by DOE. P.N.G. thanks Barrett Rogers for very illuminating discussions.

- [1] F. Wagner and ASDEX Team, Phys. Rev. Lett. **49**, 1408 (1982).
- [2] K. H. Burrell and DIII-D Team, Plasma Phys. Controlled Fusion **34**, 1859 (1992).
- [3] R. J. Groebner, Phys. Fluids B **5**, 2343 (1993).
- [4] F. M. Levinton and TFTR Team, Phys. Rev. Lett. **75**, 4417 (1995).
- [5] F. X. Söldner, Jet Team, Plasma Phys. Controlled Fusion **39B**, 353 (1997).
- [6] P. N. Guzdar, R. G. Kleva, and L. Chen, Phys. Plasmas **8**, 459 (2001).
- [7] S.-I. Itoh and K. Itoh, Phys. Rev. Lett. **60**, 2279 (1988); K. C. Shaing and E. C. Crume, Phys. Rev. Lett. **63**, 2369 (1989).
- [8] A. B. Hassam, T. M. Antonsen, Jr., J. F. Drake, and C. S. Liu, Phys. Rev. Lett. **66**, 309 (1991).
- [9] V. Rozhansky and M. Tendler, Phys. Fluids B **4**, 1877 (1992).
- [10] S. M. Mahajan and Z. Yoshida, Phys. Plasmas **7**, 635 (2000).
- [11] J. W. Connor and H. R. Wilson, Plasma Phys. Controlled Fusion **42**, R1 (2000).
- [12] P. N. Guzdar, J. F. Drake, D. McCarthy, A. B. Hassam, and C. S. Liu, Phys. Fluids B **5**, 3712 (1993).
- [13] B. Rogers, J. F. Drake, and A. Zeiler, Phys. Rev. Lett. **81**, 4396 (1998).
- [14] X. Q. Xu, R. H. Cohen, T. D. Roglien, and J. R. Myra, Phys. Plasma **7**, 1951 (2000).
- [15] W. Suttrop, V. Mertens, H. Murman, J. Neuhauser, J. Schwenzer, and the ASDEX Upgrade Team, "Operational limits for high edge density H-mode tokamak operation" (to be published).
- [16] A. E. Hubbard, R. L. Boivin, J. F. Drake, M. Greenwald, Y. In, J. H. Irby, B. N. Rogers, and J. A. Snipes, Plasma Phys. Controlled Fusion **40**, 689 (1998).
- [17] T. N. Carlstrom, K. H. Burrell, R. J. Groenber, A. W. Leonard, T. H. Osborne, and D. M. Thomas, Nucl. Fusion **39**, 1941 (1999).
- [18] I. Gruzinov, A. Das, P. Diamond, and A. Smolyakov, "Fast Zonal Field Dynamo in Collisionless Kinetic Alfvén Wave Turbulence" (to be published).
- [19] A. Zeiler, J. F. Drake, and B. Rogers, Phys. Plasmas **4**, 2134 (1997).
- [20] Liu Chen, Zhihong Lin, and Roscoe White, Phys. Plasmas Lett. **7**, 3129 (2000).